Available online at www.sciencedirect.com
ScienceDirect
Scripta Materialia 65 (2011) 440–443
Scripta MATERIALIA
www.elsevier.com/locate/scriptamat

# Imaging planar tetragonal sheets in rhombohedral $Na_{0.5}Bi_{0.5}TiO_3$ using transmission electron microscopy

R. Beanland* and P.A. Thomas

*Department of Physics, University of Warwick, Coventry CV4 7AL, UK*

Received 1 April 2011; revised 24 May 2011; accepted 26 May 2011
Available online 2 June 2011

Planar nanometre-scale inclusions in single-crystal $Na_{0.5}Bi_{0.5}TiO_3$ have been investigated using transmission electron microscopy at room temperature. In diffraction patterns, they give rise to weak extra spots and diffuse contrast. Here we show that they are visible in diffraction contrast images, giving a new route to directly observe subtly different structures in perovskites. Visibility is determined by their structure and diffraction vector. We show that single-crystal $a^-a^-a^-$ $Na_{0.5}Bi_{0.5}TiO_3$ contains an inhomogeneous distribution of nanometre-scale {0 0 1} platelets of tetragonal $a^0a^0c^+$ material.


*Keywords:* $Na_{0.5}Bi_{0.5}TiO_3$ (NBT); Transmission electron microscopy (TEM); Electron diffraction; Ferroelectric ceramics; Crystal defects

The lead-free perovskite $Na_{0.5}Bi_{0.5}TiO_3$ (NBT) and allied materials are leading contenders to replace lead-containing piezoelectrics such as $Pb_xZr_{1-x}TiO_3$ [1]. However, NBT suffers from excessive piezoelectric hysteresis and other limitations [2], and there is still some controversy in the description of average and local symmetry of this material [3–8], particularly since strong diffuse scattering [8] and splitting of peaks inconsistent with the nominal rhombohedral structure can be observed using high-resolution diffraction [6–9]. The room-temperature (RT) structure is intimately linked to the loss of symmetry which occurs as the material is cooled from its high-temperature cubic $Pm\bar{3}m$ prototypic phase. NBT is conventionally considered to pass through a tetragonal tilted perovskite $a^0a^0c^+$ P4*bm* phase between 540 and ~300 °C [10], before forming the RT phase (where the Glazer notation [11] is used to describe the tilting of oxygen octahedra in the structure). Until recently this phase has been exclusively described as having rhombohedral $a^-a^-a^-$ R3*c* phase [3], but evidence of a monoclinic structure is now starting to emerge [6,12]. The rhombohedral RT structure has doubled periodicity along all $\langle 1\,0\,0\rangle$ directions in comparison with the prototype, and is indexed here using a pseudo-cubic unit cell in which $\langle 1\,0\,0\rangle_{PC} = 2\langle 1\,0\,0\rangle_{prototype}$, and the principal axes of the unit cell meet at an angle of 89.86° [3]. To date, the complexity of diffraction data has been explained by invoking incommensurate modulations along {1 0 0} [9], as well as nanoscale {1 0 0} sheets with an $a^0a^0c^+$ [13] or $a^-a^-c^+$ [14] structure. We present here a transmission electron microscopy (TEM) analysis of single-crystal NBT, and show that {1 0 0} sheets of material with a different structure can be visualized directly using diffraction contrast images. Using invisibility criteria it is possible to distinguish between different structural models; we find that the contrast we observe is consistent with {1 0 0} $a^0a^0c^+$ platelets of material in an $a^-a^-a^-$ matrix. The ability to observe different tilt structures directly using diffraction contrast TEM gives a new tool to explore the microstructure of these technologically important materials.

Crystals of NBT were prepared using a flux growth technique [3]. TEM specimens were prepared using conventional techniques, i.e. grinding and polishing to a thickness of approx. 20 μm followed by ion milling to electron transparency. Samples were examined in a JEOL 2000FX microscope operating at 200 kV.

Micrographs showing typical domain and defect structures are shown in Figure 1. The defect structure and type was varied, with regions tens or hundreds of micrometres in size with very high defect density (often forming a cross-type morphology along {1 1 0} planes, Fig. 1a) and similar-sized regions with much lower defect density, where individual anti-phase boundaries (APBs) and twins (domain walls) were clearly visible (Fig. 1b). The highly defective regions were too complex to be analysed. However, careful examination of regions with low

* Corresponding author. E-mail: r.beanland@warwick.ac.uk

1359-6462/$ - see front matter © 2011 Acta Materialia Inc. Published by Elsevier Ltd. All rights reserved.
doi:10.1016/j.scriptamat.2011.05.031

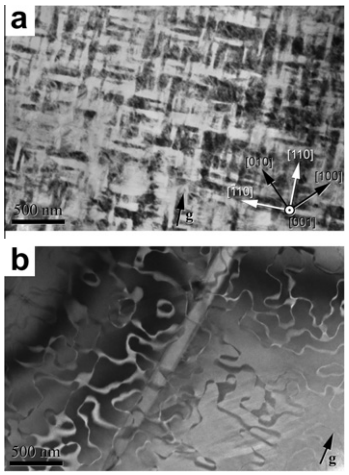


**Figure 1.** TEM micrographs of single-crystal NBT. (a) A region of high defect density with a cross-shaped ⟨1 1 0⟩ morphology (bright field, $\mathbf{g} = 220_{PC}$); (b) a region of lower defect density; individual APBs (curved) and domain walls (straight) are visible (bright field, $\mathbf{g} = 220_{PC}$).

defect densities using a variety of different **g**-vectors revealed the presence of thin plate-like defects, shown in Figure 2a. These defects were also inhomogeneously distributed; as can be seen in Figure 2a, there are regions with a high density of platelets (bottom) and others which are essentially platelet-free (top). Trace analysis showed them to lie on {1 0 0} planes. The platelets were invisible in $\mathbf{g} = 004_{PC}$, $044_{PC}$, $222_{PC}$, $224_{PC}$-type imaging conditions, as well as all-odd reflections such as $\mathbf{g} = 111_{PC}$, $113_{PC}$, etc., but had a characteristic black/white fringe contrast when imaged using $\mathbf{g} = 002_{PC}$, $024_{PC}$, $026_{PC}$ and $226_{PC}$-type reflections. This behaviour is not consistent with any twin or stacking fault vector and implies that the contrast is a form of δ fringe which arises from a different extinction distance $\xi_g$ in the platelet, i.e. indicating that it has a structure different from the matrix. Furthermore, when the faults were invisible no indication of strain contrast or the presence of a dislocation loop around the platelet could be found, implying that the crystal structure is contiguous across the defect. These properties are consistent with sheets of material with subtly different structures, for example with in-phase octahedral tilting (e.g. $a^0a^0c^+$) rather than the anti-phase $a^-a^-a^-$ tilting of the bulk structure, as proposed by Dorcet et al. [4,14] from electron diffraction data. The visibility of these regions can be understood by examining Figure 2b, which shows the difference in $\xi_g$ for different **g**-vectors in $a^-a^-a^-$, $a^-a^-a^+$ and $a^0a^0c^+$ structures. (Note that there are several different values of $\xi_g$ for each reflection in Figure 2b, since reflections which are not symmetrically equivalent in rhombohedral, orthorhombic or tetragonal structures have similar pseudo-cubic indices.) Strong δ fringes are expected when there is a large difference in $\xi_g$, particularly when $\xi_g$ in the platelet is much smaller than in the matrix (indicating that the diffracted beam is much stronger in the platelet); for example, $a^0a^0c^+$ platelets should give strong contrast when imaged using $002_{PC}$-type reflections. Conversely, the defects should be close to invisible for small differences in $\xi_g$ (e.g. $022_{PC}$).

This analysis shows that nanoscale $a^0a^0c^+$ platelets should be visible in a variety of imaging conditions, as observed in our material. The observed contrast is not consistent with $a^-a^-a^+$ tilting at {0 0 1} twin boundaries as proposed by Dorcet et al. [4,14] since this generally results in an increase in $\xi_g$ rather than a decrease, and they should only give strong contrast in $135_{PC}$ images. The observed contrast is also not consistent with sheets of Na/Bi ordering since this only affects reflections with all-odd pseudo-cubic indices (not shown on Figure 2b).

Selected area diffraction patterns (SADPs) taken from a region containing a high density of platelets (Fig. 3a) are shown in Figure 3b–d. Weak spots with pseudo-cubic indices $(h\ k\ 0)_{PC}$, where $h$ and $k$ are both odd, are visible in the [1 0 0] SADP, one of which is marked with an arrow. Although clear in this image, their intensity was very weak (~0.05% of the intensity of the 000 beam) and they were only visible because of the high dynamic range of the digital camera used. It was not possible to form images of the platelets using these extremely weak reflections. They are consistent with a small volume of material which has in-phase tilting [15]; systematic absences are expected along ⟨1 1 0⟩, marked by lines in Figure 3b [16]. In-phase tilting gives no additional spots in the [1 0 1] SADP (Fig. 3c), but strong diffuse contrast and streaking along the [1 0 0] and [0 0 1] directions is present in diffraction patterns taken along higher index

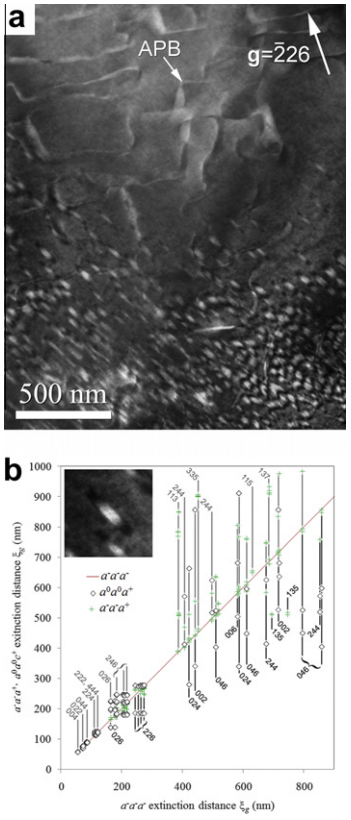


**Figure 2.** (a) Dark field, $\mathbf{g} = \bar{2}26_{PC}$ TEM micrograph showing {1 0 0} planar platelets (black/white contrast). (b) Comparison of $\xi_g$ for $a^-a^-a^-$, $a^-a^-a^+$ and $a^0a^0c^+$ structures; platelets will only have strong contrast for reflections below the red line. The inset shows an enlargement from Figure 2a. Extinction distances were calculated using JEMS [19].